

# Polar Behavior in a Magnetic Perovskite Via A-Site Size Disorder

D.J. Singh

*Materials Science and Technology Division, Oak Ridge National Laboratory, Oak Ridge, Tennessee 37831-6114*

Chul Hong Park

*Research Center for Dielectric and Advanced Matter Physics,  
Pusan National University, Busan 609-735, Korea*

(Dated: November 1, 2021)

We elucidate a mechanism for obtaining polar behavior in magnetic perovskites based on A-site disorder and demonstrate this mechanism by density functional calculations for the double perovskite (La,Lu)MnNiO<sub>6</sub> with Lu concentrations at and below 50%. We show that this material combines polar behavior and ferromagnetism. The mechanism is quite general and may be applicable to a wide range of magnetic perovskites.

PACS numbers: 77.84.Dy, 75.50.Dd

There is great interest in materials that combine magnetism and polar behavior, especially multiferroics with both ferromagnetism and ferroelectricity.<sup>1,2,3,4,5,6</sup> While there are many ferromagnets and many ferroelectrics, there remarkably few materials combining the two properties. Arguments have been made explaining this apparent incompatibility in the case of perovskite ABO<sub>3</sub> oxides.<sup>5</sup> In essence, it is because the best perovskite magnets have magnetic ions on the *B* site, while ferroelectrics, such as BaTiO<sub>3</sub>, usually have *B* site ions with no *d* electrons. Here we elucidate a mechanism for inducing polar behavior in magnetic perovskites and demonstrate this mechanism by density functional calculations for a ferromagnetic Ni-Mn double perovskite. This mechanism is quite general and may be applicable to a wide range of magnetic perovskites.

Perovskite lattice instabilities are often understood using the tolerance factor  $t = (r_O + r_A)/\sqrt{2}(r + r_B)$ , where  $r_O$ ,  $r_A$ , and  $r_B$  are the O, *A*-site and *B*-site ionic radii, respectively.<sup>18</sup> Ferroelectrics, such as BaTiO<sub>3</sub> and KNbO<sub>3</sub>, have  $t > 1$ , indicating the that *B* site ion is too small for its site in the ideal cubic structure. In the ferroelectric ground state of these so-called *B*-site driven materials, this ion off-centers, aided by hybridization with O states. There is another important class of ferroelectric perovskites, so called *A*-site driven materials. In these,  $t$  is normally less than unity, and the ferroelectricity is from off-centering of *A*-site ions. This family includes the technologically important Pb based piezoelectrics and relaxor ferroelectrics. The essential physics is lone pair stereochemistry, specifically hybridization of Pb and Bi *6p* states with O *p* states.<sup>8</sup> This class includes the few known magnetic ferroelectrics with strong ferroelectric properties, *e.g.* BiFeO<sub>3</sub>, BiMnO<sub>3</sub>, and PbVO<sub>3</sub>.<sup>9,10,11,12,13</sup> Without Pb or Bi,  $t < 1$  perovskite structures generally derive from BO<sub>6</sub> octahedral tilts and not *A*-site off-centering.

Ions with *d* electrons are generally larger than *d*<sup>0</sup> ions. The majority of magnetic perovskites have  $t < 1$ , with lattice structures based on tilts of the BO<sub>6</sub> octahedra and not ferroelectricity. However, first principles calculations have shown that, while these materials have tilted ground

states, if the octahedra are prevented from tilting, strong ferroelectricity may result, with an energy intermediate between the ideal cubic perovskite structure and the ground state structure, but closer to the later.<sup>14,15,16,17</sup> The role of Pb and Bi is then to shift the balance between these states to yield ferroelectricity. Here we use a different approach to shift the balance between these states based on *A*-site size disorder.<sup>15,16,17</sup> This is applied rare-earth double perovskites, R<sub>2</sub>MnNiO<sub>6</sub> where we obtain polar behavior combined with ferromagnetism for mixtures of large and small rare earth ions. The motivation for this choice is that the charge difference  $\delta Q=2$  between Mn<sup>4+</sup> and Ni<sup>2+</sup> and their size difference (Shannon radii,<sup>18</sup>  $r_{\text{Mn}^{4+}}=0.67\text{\AA}$ ,  $r_{\text{Ni}^{2+}}=0.83\text{\AA}$ ) indicates *B*-site ordering into the double perovskite structure,<sup>19</sup> and that La<sub>2</sub>MnNiO<sub>6</sub> and Bi<sub>2</sub>MnNiO<sub>6</sub> are known to form and to be ferromagnetic.<sup>20,21,22,23,24,25</sup> These two compounds were previously studied by first principles calculations.<sup>26,27</sup>

We used the local density approximation (LDA) in the general potential linearized augmented planewave (LAPW) method,<sup>28</sup> with well converged basis sets including local orbitals.<sup>29</sup> The LAPW sphere radii were 2.0  $a_0$  for La and Lu, 1.9  $a_0$  for Ni and Mn and 1.55  $a_0$  for O.<sup>30</sup> Mn and Ni atoms were placed in supercells with the double perovskite (rock-salt) ordering, and various orderings of the *A*-site ions. The primary results reported here were done with 40 atom supercells. However, the lattice parameter was determined by relaxation of a 10 atom cell of compositions LaLuMnNiO<sub>6</sub>. No symmetry was imposed, either for the 10 atom or 40 atom cells, but for the 40 atom cells the lattice parameters were held fixed at their pseudocubic values as determined from the relaxation of the 10 atom ferromagnetic cell, which as shown in Fig. 1 was 3.75 Å. For both the parallel and antiparallel spin alignments, relaxation of the 10 atom cells yielded structures with off-centering of the Lu ions, *i.e.* polar structures, even though perovskite R<sub>25</sub> type tilts are allowed in this cell.

Our electronic structure for (La,Lu)MnNiO<sub>6</sub> is similar to those previously found for the Bi and La

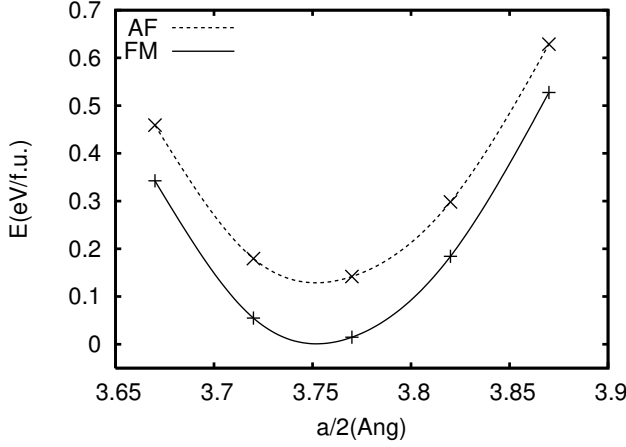


FIG. 1: Energy of 10 atom LaLuMnNiO<sub>6</sub> cells vs. pseudocubic lattice parameter ( $a/2$ ) for parallel (FM) and antiparallel (AF) Ni and Mn moments. Note that the FM alignment is strongly favored.

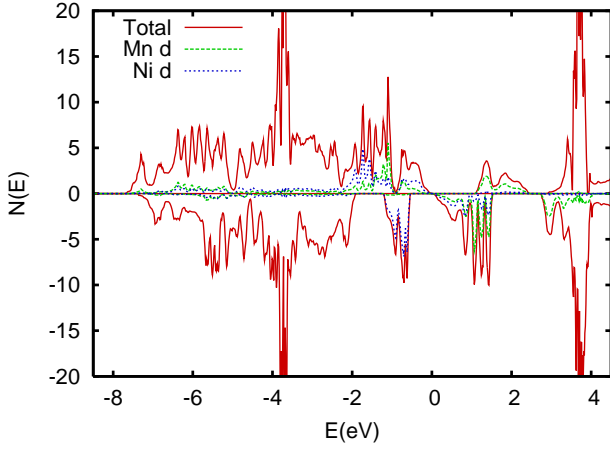


FIG. 2: (color online) Electronic density of states of a 10 atom ferromagnetic LaLuMnNiO<sub>6</sub> cell ( $a=3.77\text{\AA}$ ). The peaks at  $\sim -3.7\text{ eV}$  and  $\sim 3.7\text{ eV}$  are the Lu and La  $f$  states, respectively. The projections are onto LAPW spheres.

analogues,<sup>26,27</sup> and show high spin  $\text{Mn}^{4+}$  and  $\text{Ni}^{2+}$ . The LDA density of states for the relaxed ferromagnetic structure at  $a=3.77\text{\AA}$  is shown in Fig. 2, and schematically in Fig. 3. For the various supercells we find either very small gaps or small band overlaps in the LDA depending on the exact crystal structure. We also performed some LDA+ $U$  calculations (not shown). These yield insulating band structures, with gaps depending on  $U$ . Near metallicity is highly unfavorable for ferroelectricity, as it means strong electronic dielectric screening that will weaken the Coulomb interactions. Nonetheless, we use the LDA to avoid the ambiguity associated with an adjustable parameter ( $U$ ) and expect that the prediction of polar behavior will be robust.

The ferromagnetism is due to the fact that with parallel alignments of the Mn and Ni spins there is a strong

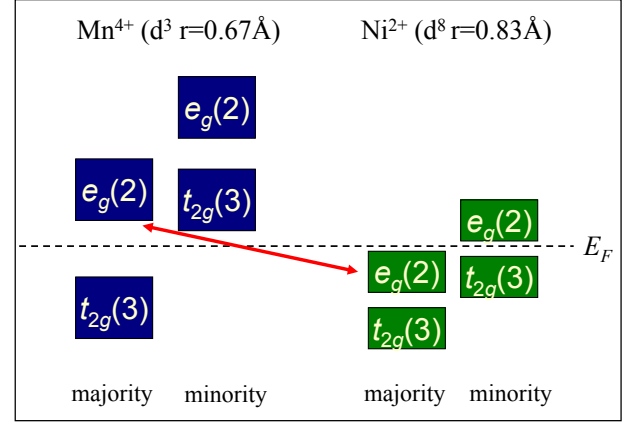


FIG. 3: (color online) Schematic depiction of the electronic structure of LaLuMnNiO<sub>6</sub> showing the dominant superexchange coupling by the arrow.

TABLE I: Lu displacements for the various supercells.  $|\langle \delta \rangle|$  is the magnitude of the average Lu displacement, and  $\langle |\delta| \rangle$  is the average magnitude.

| $n_{\text{La}}$ | $n_{\text{Lu}}$ |     | $\langle \delta \rangle$ | $\langle  \delta  \rangle$ | $ \langle \delta \rangle  / \langle  \delta  \rangle$ |
|-----------------|-----------------|-----|--------------------------|----------------------------|---|
| 4               | 4               | "G" | 0.243Å                   | 0.396Å                     | 0.61  |
| 4               | 4               | "A" | 0.405Å                   | 0.414Å                     | 0.98  |
| 4               | 4               | "C" | 0.013Å                   | 0.396Å                     | 0.04  |
| 4               | 4               | "P" | 0.201Å                   | 0.403Å                     | 0.48  |
| 5               | 3               |     | 0.379Å                   | 0.379Å                     | 1.00  |
| 6               | 2               |     | 0.331Å                   | 0.331Å                     | 1.00  |

cross-gap hybridization of the unoccupied  $e_g$  majority states of  $\text{Mn}^{4+}$  with the occupied majority  $e_g$  states of  $\text{Ni}^{2+}$ , leading to a ferromagnetic coupling consistent also with the Goodenough-Kanamori rules.<sup>31,32,33</sup> This ferromagnetic superexchange is particularly strong because in perovskites the strongest coupling through the near linear  $B\text{-O-B}$  bonds is via  $e_g - p_\sigma$  hopping. The strength of this coupling is evident from the sizable crystal field splittings<sup>34</sup> of both the Mn and Ni  $d$  states (Fig. 2). Thus the hybridization between occupied and unoccupied  $e_g$  orbitals, allowed for ferromagnetic alignment, but not for antiferromagnetic alignment, strongly favors ferromagnetism. Since the hopping is mediated by O this is not direct exchange, like the weak ferromagnetic coupling generally associated with the Goodenough-Kanamori ferromagnetism, but is a conventional strong superexchange.<sup>33,35,36</sup>

While our relaxed structure for the 10 atom cell is polar, this size supercell favors ferroelectricity (ferroelectricity arises from a zone center instability, while the competing tilt modes occur at the zone boundary and a 10 atom cell restricts tilts to the  $R$ -point). We therefore performed supercell calculations with a  $2 \times 2 \times 2$  40 atom supercell. This cell is doubled along the  $[001]$ ,  $[011]$  and  $[111]$  directions and so allows arbitrary mixtures of

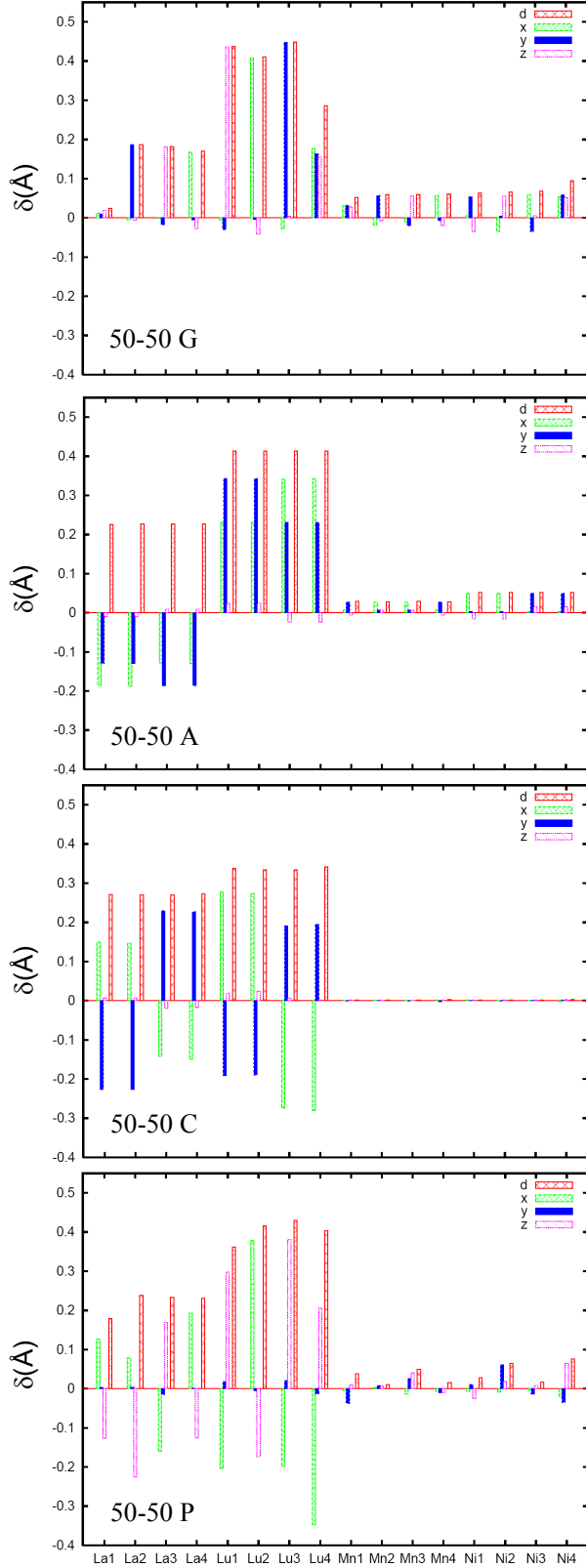


FIG. 4: (color online) Cation displacements with respect to their O cages in a 40 atom relaxed supercells of composition  $(\text{La}_{0.5}\text{Lu}_{0.5})\text{MnNiO}_6$ .

tilt instabilities and accommodates the observed Glazer patterns of perovskite tilt systems.<sup>37</sup>

As mentioned, all supercells were for the double perovskite structure, *i.e.* rock-salt ordering of the *B*-site Ni and Mn ions. For the *A*-site, we considered four arrangements of the Lu and La at a 50–50 composition as well as one supercell each for 5/8–3/8 and 3/4–1/4 compositions. The specific cells at the 50–50 composition were (1) rock-salt ordering of La and Lu (“G” in the following), (2) (001) layers of La and Lu (“A”), (3) lines of La and Lu along [001] and ordering  $c(2 \times 2)$  in plane (“C”) and (4) a cell maximizing like near neighbors (La at corner and edge centers, Lu at face and body centers, denoted “P”). The 5/8–3/8 supercell was constructed by replacing one Lu by La in the cell “G”, while the 75–25 supercell was made by substitution of two Lu by La in the same “G” supercell.

Fig. 4 shows the cation positions in the lowest energy relaxed structures for the 50% Lu supercells with respect to the centers of their nearest neighbor O cage (nearest 12 O atoms for the *A*-site atoms, and nearest 6 O for the *B*-sites ions). The average displacements of the Lu for the various cells are summarized in Table I. As may be seen, in all cases Lu strongly off-centers, by on average  $\sim 0.4\text{\AA}$  for the 50–50 supercells and slightly less for the lower concentration cells. Interestingly, unlike other *A*-site driven perovskite ferroelectrics,<sup>38</sup> there is very little off-centering of the *B*-site ions. In fact the largest off-centering aside from Lu are of the La ions and depending on the supercell these may or may not be parallel to the Lu.

The individual Lu off-centerings tend to avoid [111] and equivalent directions, and also tend to be non-collinear with each other for 50% Lu concentration, *e.g.* in the “G” ordering (nominally the highest symmetry case), three of the Lu displace along different Cartesian directions, while the fourth has a smaller displacement near [111]. A preference for Cartesian directions was noted in  $(\text{K,Li})\text{NbO}_3$ ,<sup>16</sup> and understood from the fact that the square faces of the cage (the faces with the most room for the Li ion) are along these directions. Turning to the question of polar behavior, both of the cells at less than 50% Lu concentration show polar structures. At 50% the cells “G”, “P” and “A” have polar structures, most strongly so for “G”, while “C” is nearly antiferrodistortive, with tilts that avoid compressing the O - La bonds. Of the four supercells investigated the relaxed “G” structure had the highest energy. Taking this energy as the zero, the calculated energies were -0.43 eV, -0.36 eV, and -0.42 eV, for “A”, “C” and “P”, respectively on a per formula unit (10 atom) basis. The similarity of the energies other than “G” show that the *A*-site ions will be disordered in material made by conventional methods, in agreement with what would normally be expected in perovskites with chemically similar, same charge, ions. While in the ordered “C” structure structure a long range tilt pattern of this type is allowed, this will not be the case in general for disordered *A*-site ions.

Assuming that the  $A$ -sites are disordered in the alloy, this dependence of polar behavior on chemical ordering is more consistent with relaxor ferroelectric behavior than normal ferroelectricity.<sup>39,40,41</sup> However, it should be kept in mind that the relaxations reported here were performed within the LDA, which also predicts zero or very small band gaps, while in reality larger, but unknown gaps may be present. Larger gaps would lower the electronic dielectric constant favoring ferroelectricity and stronger coupling between the Lu off-centerings. While actual ferroelectricity may occur, what can be concluded here is that polar behavior will occur in disordered  $(\text{La,Lu})\text{MnNiO}_6$  for Lu concentrations at or below 50%. This may be ferroelectricity or relaxor ferroelectricity.

This polar behavior arises because of frustration of the tilt instabilities due to the mixture of  $A$ -site cation sizes and the fact that the coherence length for off-centering of  $A$ -site ions is shorter than that for the tilt instabilities. This mechanism is quite general in principle, may be useful in producing polar behavior in other perovskites.

Qualitatively, this is related to the rigidity of the  $\text{BO}_6$  octahedra. This condition is often but not always met, as for example, while often tilt instabilities are strengthened by pressure, there are cases where this does not hold.<sup>42</sup>

It may be difficult to synthesize perovskite  $(\text{La,Lu})_2\text{MnNiO}_6$  due to phase separation<sup>43</sup> or competing phases, *e.g.* tungsten bronze as often occurs with mismatched  $A$ -sites. These issues can sometimes be overcome using thin film techniques, such as pulse laser deposition, or by high pressure synthesis, which favors the high density perovskite structure. Further, polar behavior is predicted over a wide composition range. This may help in finding specific compositions amenable to synthesis. In any case, the proposed mechanism is quite general, and should apply to other mixtures of  $A$ -site ions with different size, *e.g.* La with other small rare earths.

This work was supported by the Department of Energy, Division of Materials Science and Engineering and the Office of Naval Research.

- <sup>1</sup> D.N. Astrov, JETP **11**, 708 (1960).
- <sup>2</sup> V.J. Folen, G.T. Rado, and E.W. Stalder, Phys. Rev. Lett. **6**, 607 (1961).
- <sup>3</sup> M. Fiebig, Th. Lottermoser, D. Frohlich, A.V. Goltsev, and R.V. Pisarev, Nature (London) **419**, 818 (2002).
- <sup>4</sup> W. Eerenstein, N.D. Mathur, and J.F. Scott, Nature **442**, 759 (2006).
- <sup>5</sup> N.A. Hill, J. Phys. Chem. B **104**, 6694 (2000).
- <sup>6</sup> N.A. Spaldin and M. Fiebig, Science **309**, 391 (2005).
- <sup>7</sup> G.A. Samara, T. Sakudo, and K. Yoshimitsu, Phys. Rev. Lett. **35**, 1767 (1975).
- <sup>8</sup> R.E. Cohen, Nature **358**, 136 (1992).
- <sup>9</sup> R.T. Smith, G.D. Achenbach, R. Gerson, and W.J. James, J. Appl. Phys. **39**, 70 (1968).
- <sup>10</sup> G.A. Smolenskii, and I. Chupis, Sov. Phys. Usp. **25**, 475 (1982).
- <sup>11</sup> H. Chiba, T. Atou, and Y. Syono, J. Solid State Chem. **132**, 139 (1997).
- <sup>12</sup> R.V. Shpanchenko, V.V. Chernaya, A.A. Tsirlin, P.V. Chizhov, D.E. Sklovsky, E.V. Antipov, E.P. Khlybov, V. Pomjakushin, A.M. Balagurov, J.E. Medvedeva, E.E. Kaul and C. Geibel, Chem. Mater. **16**, 3267 (2004).
- <sup>13</sup> A.A. Belik, M. Azuma, T. Saito, Y. Shimakawa, and M. Takano, Chem. Mater. **17**, 269 (2005).
- <sup>14</sup> S.V. Halilov, M. Fornari, and D.J. Singh, Appl. Phys. Lett. **81**, 3443 (2002).
- <sup>15</sup> D.J. Singh, M. Ghita, S.V. Halilov and M. Fornari, J. Phys. IV (Paris) **128**, 47 (2005).
- <sup>16</sup> D.I. Bilc and D.J. Singh, Phys. Rev. Lett. **96**, 147602 (2006).
- <sup>17</sup> D.J. Singh, M. Ghita, M. Fornari, and S.V. Halilov, Ferroelectrics **338**, 73 (2006).
- <sup>18</sup> R.D. Shannon, Acta Cryst. **A32**, 751 (1976).
- <sup>19</sup> M.T. Anderson, K.B. Greenwood, G.A. Taylor, and K.R. Poeppelmeier, Prog. Solid State Chem. **22**, 197 (1993).
- <sup>20</sup> J.B. Goodenough, A. Wold, R.J. Arnett, and N. Menyuk, Phys. Rev. **124**, 373 (1961).
- <sup>21</sup> G. Blasse, J. Phys. Chem. Solids **26**, 1969 (1965).
- <sup>22</sup> M. Azuma, K. Takata, T. Saito, S. Ishiwata, Y. Shimakawa, and M. Takano, J. Am. Chem. Soc. **127**, 8889 (2005).
- <sup>23</sup> H. Hughes, M.M.B. Allix, C.A. Bridges, J.B. Claridge, X. Kuang, H. Niu, S. Taylor, W. Song, and M.J. Rosseinsky, J. Am. Chem. Soc. **127**, 13790 (2005).
- <sup>24</sup> N.S. Rogado, J. Li, A.W. Sleight, and M.A. Subramanian, Adv. Mater. **17**, 2225 (2005).
- <sup>25</sup> M. Sakai, A. Masuno, D. Kan, M. Hashisaka, K. Takata, M. Azuma, M. Takano, and Y. Shimakawa, Appl. Phys. Lett. **90**, 072903 (2007).
- <sup>26</sup> Y. Uratani, T. Shishidou, F. Ishii, and T. Oguchi, Physica B **383**, 9 (2006).
- <sup>27</sup> S.F. Mater, M.A. Subramanian, A. Villesuzanne, V. Eyert, and M.H. Whangbo, J. Magn. Magn. Mater. **308**, 116 (2007).
- <sup>28</sup> D.J. Singh and L. Nordstrom, *Planewaves, Pseudopotentials and the LAPW Method, 2nd. Ed.* (Springer, Berlin, 2006).
- <sup>29</sup> D. Singh, Phys. Rev. B **43**, 6388 (1991).
- <sup>30</sup> Smaller radii of  $1.53a_0$  for O and  $1.88a_0$  for the  $B$ -site ions were used in some relaxations to avoid overlapping spheres. The results for different radii were cross-checked.
- <sup>31</sup> J.B. Goodenough, Phys. Rev. **100**, 564 (1955); J. Phys. Chem. Solids **6**, 287 (1958).
- <sup>32</sup> J. Kanamori, J. Phys. Chem. Solids **10**, 87 (1959).
- <sup>33</sup> J.B. Goodenough, *Magnetism and the Chemical Bond* (Wiley, New York, 1963).
- <sup>34</sup> Crystal field splittings are mainly from hybridization of metal  $d$  and O  $p$  states in perovskites, *i.e.* the nominal  $d$  bands are anti-bonding combinations of  $d$  and  $p$  states so since the hybridization is stronger for the  $e_g$ - $p_\sigma$  than for the  $t_{2g}$ - $p_\pi$  combination, the  $e_g$  states are higher in energy. Large crystal field splittings show strong hybridization.
- <sup>35</sup> Note the exchange splitting of O  $p$  bands (Fig. 2), which shows the involvement of O via hybridization.

- <sup>36</sup> P.W. Anderson, Phys. Rev. **115**, 2 (1959).
- <sup>37</sup> A.M. Glazer, Acta Cryst. B **28**, 3384 (1972).
- <sup>38</sup> M. Ghita, M. Fornari, D.J. Singh, and S.V. Halilov, Phys. Rev. B **72**, 054114 (2005).
- <sup>39</sup> G.A. Smolenski and V.A. Isupov, Dokl. Akad. Nauk. SSR **97**, 653 (1954).
- <sup>40</sup> G. Burns and F.H. Dacol, Phys. Rev. B **28**, 2527 (1983).
- <sup>41</sup> G.A. Samara, J. Phys. Condens. Matter **15**, R367 (2003).
- <sup>42</sup> R.J. Angel, J. Zhao, and N.L. Ross, Phys. Rev. Lett. **95**, 025503 (2005).
- <sup>43</sup> S. Park, N. Hur, S. Guha, and S.W. Cheong, Phys. Rev. Lett. **92**, 167206 (2004).